Objective Evaluation of Body Displacements during Activities using The Wearable Inertial System ActimedARM

Julien Collet[1], Martin Cerny[2], Ludovic Delporte[3], Norbert Noury[1]

Abstract— **This paper presents an algorithm for the objective assessment of the motion of a body during health-evaluation physical tests using our inertial sensor, namely the ActimedARM. With the orientation quaternions provided by the sensor and integrating twice the calibrated acceleration measurements, we are able to compute the displacement of the sensor worn by a patient. To validate our data we have made measurements with both our sensor and a reference optical system. The displacement curves provided by our algorithm were correlated to the gold-standard system with a mean rate of 94.96%.**

Index Terms— **Actimetry monitoring, inertial sensors, sit-to-stand test, quaternion, embedded systems.**

I. INTRODUCTION

Physical exercises can help diagnosing diseases affecting the overall health condition. For example, diseases such as chronic obstructive pulmonary diseases (COPD) can be efficiently diagnosed by the study of the physical activity of a patient. Therefore, normalized activity estimation tests were developed, such as the chair-rise test (CRT) that can help estimates the evolution of post operation rehabilitation on a patient or the physical condition of the elderly [1]. Nowadays, gold-standard systems can be used for the objective study of these exercises.

Typical gold-standard systems for motion evaluation are composed of sets of cameras. These kinds of systems can give precise description of the patient motion by the means of tags placed on the body or with the help of complex image processing algorithms. But these tremendous performances imply important and restrictive drawbacks such as the need for high-performance computational systems and to wear physical tags which is hardly acceptable in daily life.

Recent works and achievements in the MEMS industry made possible the design of small integrated wearable sensors for home health monitoring that are thereby more acceptable for the patient. We used a sensor we developed, the ActimedARM [2], to monitor activities (postures, transfer and walk) and wanted to use it for the objective assessment of the displacement during sit-to-stand tests.

The goal of our study is to provide an objective tool that can be used by patients in their own environment for the monitoring of their motion during physical exercises.

[1] Julien Collet and Prof. Norbert Noury are with lab. Institute of Nanotechnology of Lyon INL-UMR5270, CNRS, INSA Lyon, Villeurbanne, F-69621, France (**julien.collet@cpe.fr** and **norbert.noury@insa-lyon.fr**)

[2] Martin Cerny is with VSB Technical University Ostrava, Ostrava, Czech Republic, supported by the project Opportunity for young researchers, reg. no. CZ.1.07/2.3.00/30.0016 (**martin.cerny@vsb.cz**)

[3] Ludovic Delporte is with CRNL (**ludovic.delporte@chu-lyon.fr**)

II. MATERIALS AND METHOD

A. Material

The ActimedARM was used to measure the acceleration of a body. This system is composed of a 32-bit ARM microcontroller, a three-axis accelerometer, a three axis magnetometer, a SD card and a 802.15.4 wireless module. The ActimedARM can measure the acceleration and the intensity of the magnetic field along its three axis and detect events (walking episodes, transfers, postures). It also performs a low-pass filtering on the acceleration data to remove high-frequency noise [2].

The ActimedARM can compute on-board the quaternion equivalent to the orientation of the person wearing the system using the acceleration of the gravity and the measurement of the magnetic field. As to represent orientation, quaternions are more interesting than Euler angles despite their relative obfuscated representation because they are smaller —and thereby more easily embedded— and also because they do not present singularities unlike Euler angles [3].

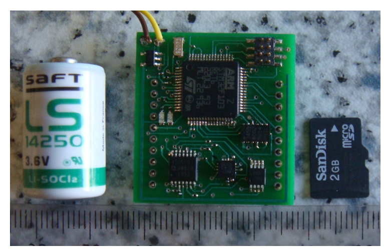

Fig. 1. The wearable actimeter used for experimentations: ActimedARM (center), battery (left) and SDCard (right).

The sensor can be used in both data-logging and data-pushing modes. In the first mode, the 802.15.4 module (XBee) can stream the measured data to an host computer running a python software able to show real-time person orientation and display events on screen. In this mode, the autonomy is 24 days (resp. 8 days) on 3600 mAh battery (resp. 1200 mAh) [2]. When used as a data-logger, the embedded communication module is turned off to increase battery life allowing autonomy greater than 32 days (3600mAh). The data are then written on the memory card for offline analysis [2].

B. Implementation

1) Overall description of the algorithm: The algorithm is divided into two individual parts, the correction of the orientation error and the computation of displacement and velocity from the acceleration:

978-1-4244-7929-0/14/$26.00 ©2014 IEEE

1. Correction of the placement orientation
2. Velocity computation process
   - High-pass filter
   - Integration
3. Displacement computation process
   - Integration
   - High-pass filter

The first step is dedicated to the correction of the difference between the referential of the body, measured by the sensor, and the terrestrial reference frame.

The second and third steps produce the displacement values from the corrected acceleration measurements. The numerical high-pass filters are used to overcome the need for initial conditions during the entire integration process [4].

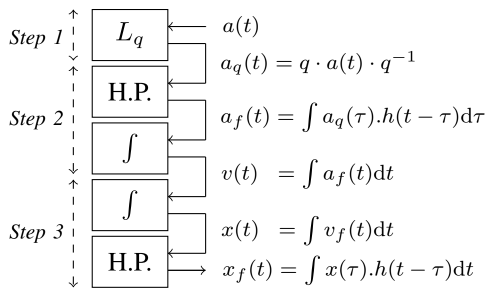

Fig. 2. Global schematic of the algorithm where $a(t)$ is the raw acceleration input signal and $x_f(t)$ is the output processed position signal.

2) Orientation error corrections using quaternion: As it is placed manually onto the patient's body, the sensor is poorly aligned with common reference, resulting in a constant orientation error. This orientation offset error can be seen as a rotation between the sensor and the terrestrial reference frame. The orientation is available and given under the form of a quaternion by the sensor at each time. Knowing this, it is thus possible to project the signals in the initial referential by applying the inverse transform.

The idea behind this recalibration is to re-project the acceleration signals along the three axis of the terrestrial reference. This operation is mathematically defined by the following relationship for a given acceleration sample $\mathbf{a}_n$, in the reference frame $\langle i, j, k\rangle$ of the sensor, a transformation operator $\mathbf{L}_q$ and the output sample $\mathbf{a}'_n$, in the terrestrial reference frame $\langle i', j', k'\rangle$:

$$\mathbf{a}'_n = \mathbf{L}_q \cdot \mathbf{a}_n = q \cdot \mathbf{a}_n \cdot q^{-1} \tag{1}$$

The Hamilton product, which defines the multiplication between two quaternions, is not commutative and defined by (7). Coordinate changes and relationship between rotations and quaternions are also discussed in Appendix.

The input and output samples are written under the form of a pure quaternion (i.e. with null real part):

$$\mathbf{a}_n = \begin{bmatrix} 0 \\ \hline a_i \\ a_j \\ a_k \end{bmatrix} \quad \mathbf{a}'_n = \begin{bmatrix} 0 \\ \hline a_{i'} \\ a_{j'} \\ a_{k'} \end{bmatrix} \tag{2}$$

The quaternion q is the unit quaternion (a versor) holding the rotation to be applied —the inverse of the orientation measured— and q^{-1} is its inverse quaternion. This quaternion must be carefully chosen in order to accurately recalibrate the data.

Depending on the context of the analysis (real-time vs. offline), there are two ways of finding the most accurate quaternion. During *a posteriori* analysis, a good strategy is to detect an initial standing position as a referential and to compute the quaternion. For real-time embedded perspective, on-line detection of standing posture can be developed with further manual or automatic calibration routines.

3) Numerical integration: Numerical integration of signals is central in our algorithm so we had to investigate and compare several numerical methods:

- *Rectangle rule*:

$$y[n] = \frac{1}{f_s}\sum_{k=0}^{n} x[n-k] = y[n-1] + \frac{1}{f_s}x[n]$$

- *Trapezoidal rule*:

$$y[n] = y[n-1] + \frac{1}{2f_s}\left(x[n-1] + x[n]\right)$$

- *Simpson's rule*:

$$y[n] = y[n-1] + \frac{1}{f_s} \cdot \frac{x[n-1] + 4.x[n] + x[n+1]}{6}$$

Where $x[n]$ (resp. $y[n]$) represent the n-th input (resp. output) sample and f_s is the sampling frequency.

We have chosen to use the trapezoidal rule because it is the best algorithm in terms of performance and computation weight. While the rectangle rule is the easiest to implement, it is the less accurate. The Simpson algorithm, in comparison with the trapezoidal rule is not more precise and generates a computational overhead [4][5].

4) Filters characteristics: Two types of numerical filters were considered, the first one being an Infinite Impulse-Response (IIR) filter and the other, a Finite Impulse-response (FIR) filter. We have chosen to process our data using FIR filters because its phase response is linear. However, they have higher order than IIR for a given cut-off frequency implying longer transient in the result signal.

C. Experiments

In order to evaluate the accuracy of the algorithm, experiments were conducted with an ActimedARM (sampling frequency: 25Hz) and a gold-standard video system composed of 7 Eagle-type cameras (resolution: 1.3M pixels, sampling frequency: 200Hz) from Motion Analysis Inc. (Santa Rosa, CA USA). A total of 13 tags were placed on the body of the subjects for the evaluation of the motion by the cameras. One actimedARM was placed near the navel, with a tag placed on it and another on the pelvis, as shown in Fig. 3.

The experimental protocol involved 4 male subjects (36 ± 11.5yrs, 87.7 ± 32.57kg,1.73 ± 0.10m), performing different tasks of a normal activity (e.g. standing up, sitting down

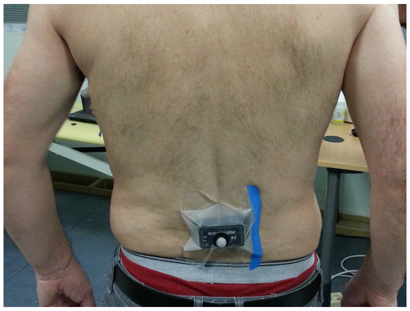

Fig. 3. Placement of one ActimedARM and its tag, near the pelvis.

and walking). We were comparing the positions given by the video system to the one computed by our inertial sensors. For the sake of simplification, we present here only the results in sit-to-stand, because the z axis is less sensitive to misorientations.

The scenario precisely consisted in a vertical jump, ten seconds before the start of the record in order to synchronize the signals, followed by 9 sit-to-stands sequences. Two signals were extracted from the video for each experiment: one representing the displacements along the vertical axis of the tag placed on the sensor and another one placed on the navel. The filter used during processing was a high-order FIR filters with a very low cut-off frequency which was adapted to the experimental conditions.

D. Results

With regards to the results we obtained, we found that the sensor placed on the navel was relatively accurate. In Fig. 4 are shown two position signals extracted from the set of cameras (one tag on the pelvis and the other near navel), the raw data from the ActimedARM located on the pelvis and the processed data from this same sensor.

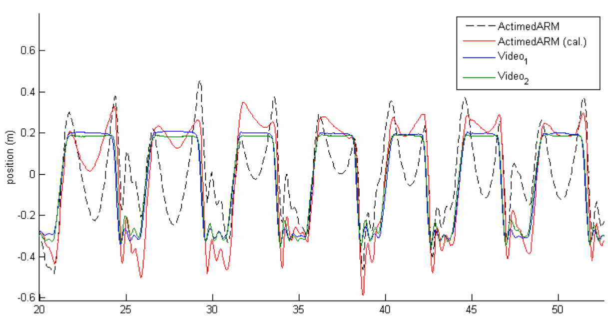

Fig. 4. Experiment #1 — Signals along vertical axis collected during a serie of Sit-to-Stand and Back-To-sit, raw signal extracted from the ActimedARM (dashed), corrected signal (red) and signals extracted from video systems (blue, green)

The gain in terms of accuracy can be appreciated on this figure when comparing the uncorrected position signal from the ActimedARM (Sensor (raw)) and the quaternion-corrected signal (Sensor (cal.)). This improvement is also supported by the correlation matrices shown in Table 1, 2 and 3. The correlation coefficients between the uncorrected signal from experiment #1 (resp. #2 and #3) and the video systems are respectively 0.5391 (-0.2803 and -0.8497) and 0.5908 (-0.1949 and -0.7981).

When correlating video systems with the calibrated data, these coefficients are 0.9355 (0.9580 and 0.9553) and 0.9446 (0.9038 and 0.9067) denoting a significant improvement in the correlation of our signals to the video-based data.

TABLE I
CORRELATION MATRIX (EXPERIMENT #1)

	Sensor (raw)	Sensor (cal.)	Video$_1$	Video$_2$
Sensor (raw)	1.0	0.7034	0.5391	0.5908
Sensor (cal.)	0.7034	1.0	0.9355	0.9446
Video$_1$	0.5391	0.9355	1.0	0.9950
Video$_2$	0.5908	0.9446	0.9950	1.0

Gender: Male, Age: 31, Height: 1m85 , Weight: 125kg

TABLE II
CORRELATION MATRIX (EXPERIMENT #2)

	Sensor (raw)	Sensor (cal.)	Video$_1$	Video$_2$
Sensor (raw)	1.0	-0.4347	-0.2803	-0.1949
Sensor (cal.)	-0.4347	1.0	0.9580	0.9038
Video$_1$	-0.2803	0.9580	1.0	0.9603
Video$_2$	-0.1949	0.9038	0.9603	1.0

Gender: Male, Age: 54, Height: 1m70 , Weight: 65kg

TABLE III
CORRELATION MATRIX (EXPERIMENT #3)

	Sensor (raw)	Sensor (cal.)	Video$_1$	Video$_2$
Sensor (raw)	1.0	-0.8306	-0.8497	-0.7981
Sensor (cal.)	-0.8306	1.0	0.9553	0.9067
Video$_1$	-0.8497	0.9553	1.0	0.9440
Video$_2$	-0.7981	0.9067	0.9440	1.0

Gender: Male, Age: 23, Height: 1m65 , Weight: 73kg

Unfortunately, the displacement data extracted from the video were corrupted for the fourth subject, we therefore could not oppose them to the signals from the ActimedARM.

III. CONCLUSIONS

This paper shows that first assessments of the vertical motion of a patient during sit-to-stand exercises is feasible with wearable sensors, despite errors of integration and needs for regular recalibrations. This makes our sensor, with its integrated algorithm, an interesting tool for home-monitoring of the activity.

Future work will be focused on the improvement of the algorithm in order to increase its accuracy by improved signal-calibration techniques. Correcting the integration error on a regular basis by using zero-velocity update techniques could be an interesting and useful investigation way that have already been used in other contexts [5].

The impact of the sensor location should be investigated to select the best location both in terms of acceptability and quality of measurements. Also, extended experiments should be conducted to validate the application of this algorithm to other kinds of motions.

The design of the algorithm is driven by considerations of embeddability, as it could be another feature of the ActimedARM for personal, daily activity monitoring for our system. Moreover, the use of quaternions for orientation representation and calibration tends to be unavoidable as they are efficient both in computational and mathematical terms (i.e. small memory usage and no gimbal lock in comparison with Euler's angles). It is more than conceivable that the trapezoidal method will be used in the embedded version of the algorithm concerning its performances and the computational effort required. Eventually, FIR filters would be used because they can be used for real-time assessment of the motion but IIR filters should not be excluded if their loss of linear phase can be compensated because they tend to have smaller orders.

Finally, the application of this algorithm for the objective evaluation of the walk is to be investigated and could be of great importance for an overall estimation of an individual's activity.

ACKNOWLEDGMENT

The authors gratefully thank the members of team IMPACT at CRNL for accessing their MouvHandi motion platform.

APPENDIX

A. Mathematics

1) Projection and rotation: Let $a(t)$ be the acceleration measured in $\langle i, j, k\rangle$, the orthogonal sensor referential. The acceleration can be expressed, in the referential of the individual, as:

$$\begin{aligned} a(t) &= a(t)\cdot\mathbf{i} + a(t)\cdot\mathbf{j} + a(t)\cdot\mathbf{k} \\ &= a_{\mathbf{i}}(t) + a_{\mathbf{j}}(t) + a_{\mathbf{k}}(t) \end{aligned}$$

With $a_i(t)$, $a_j(t)$ and $a_k(t)$, the actual acceleration values along each base vectors of the referential. We can now decompose $a(t)$ in $\langle i', j', k'\rangle$, the orthogonal terrestrial reference frame by using the dedicated projection operator:

$$\begin{aligned} a'(t) &= \mathbf{L}'\cdot a(t) \\ &= a(t)\cdot\mathbf{i}' + a(t)\cdot\mathbf{j}' + a(t)\cdot\mathbf{k}' \\ &= a_{\mathbf{i}'}(t) + a_{\mathbf{j}'}(t) + a_{\mathbf{k}'}(t) \end{aligned}$$

In terms of measurements, the sensor can measure $a_i(t)$, $a_j(t)$ and $a_k(t)$ which are the components of the acceleration along the sensor basis vectors. We want to compute $a_{i'}(t)$, $a_{j'}(t)$ and $a_{k'}(t)$ the orthogonal components of the acceleration along each axis of the terrestrial reference frame. For example, let $a_{\mathbf{i}'}(t)$ be expressed by the combination of measured values:

$$\begin{aligned} a_{i'}(t) &= a(t)\cdot\mathbf{i}' \\ &= (a_i(t)\cdot\mathbf{i} + a_j(t)\cdot\mathbf{j} + a_k(t)\cdot\mathbf{k})\cdot\mathbf{i}' \\ &= a_i(t)\cdot\mathbf{i}\cdot\mathbf{i}' + a_j(t)\cdot\mathbf{j}\cdot\mathbf{i}' + a_k(t)\cdot\mathbf{k}\cdot\mathbf{i}' \\ &= a_i(t).cos\,\theta_{i'i} + a_j(t).cos\,\theta_{i'j} + a_k(t).cos\,\theta_{i'k} \end{aligned}$$

With $\mathbf{i}\cdot\mathbf{i}'$, $\mathbf{j}\cdot\mathbf{i}'$ and $\mathbf{k}\cdot\mathbf{i}'$ representing the projections of the basis vectors of the sensor frame into the terrestrial frame, $\mathbf{i}'$. Thus, applying this to the other measured components of the acceleration leads to the following relationships:

$$a_{i'}(t) = a_i(t).cos\,\theta_{i'i} + a_j(t).cos\,\theta_{i'j} + a_k(t).cos\,\theta_{i'k} \quad (3)$$
$$a_{j'}(t) = a_i(t).cos\,\theta_{j'i} + a_j(t).cos\,\theta_{j'j} + a_k(t).cos\,\theta_{j'k} \quad (4)$$
$$a_{k'}(t) = a_i(t).cos\,\theta_{k'i} + a_j(t).cos\,\theta_{k'j} + a_k(t).cos\,\theta_{k'k} \quad (5)$$

Where $\theta_{e'e}$ is the angle between base vectors e' of the final reference frame and e of the origin reference frame. This can therefore be noted $\mathbf{a}'(t) = \mathbf{L}'\cdot\mathbf{a}(t)$, or :

$$\begin{bmatrix} a_{\mathbf{i}'}(t) \\ a_{\mathbf{j}'}(t) \\ a_{\mathbf{k}'}(t) \end{bmatrix} = \begin{bmatrix} cos\,\theta_{i'i} & cos\,\theta_{i'j} & cos\,\theta_{i'k} \\ cos\,\theta_{j'i} & cos\,\theta_{j'j} & cos\,\theta_{j'k} \\ cos\,\theta_{k'i} & cos\,\theta_{k'j} & cos\,\theta_{k'k} \end{bmatrix} \cdot \begin{bmatrix} a_{\mathbf{i}}(t) \\ a_{\mathbf{j}}(t) \\ a_{\mathbf{k}}(t) \end{bmatrix}$$

In the case of a rotation around the base vector $\mathbf{k}$ by an angle θ, (3) (4) and (5) lead to these relationships [3]:

$$\begin{aligned} a_{i'}(t) &= a_i(t).cos\,\theta - a_j(t).sin\,\theta \\ a_{j'}(t) &= a_i(t).sin\,\theta + a_j(t).cos\,\theta \\ a_{k'}(t) &= a_k(t) \end{aligned}$$

2) Quaternions: The conjugate of a quaternion q is defined by the following relationships (With $i.j.k = -1.$):

$$q^* = \left[\begin{array}{c} q_0 \\ \hline \\ -\mathbf{q} \\ \\ \end{array}\right] = \left[\begin{array}{c} q_0 \\ \hline -q_1.i \\ -q_2.j \\ -q_3.k \end{array}\right] \quad (6)$$

The product of two quaternion q and p is partially anti-commutative and can be expressed:

$$q.p = \left[\begin{array}{c} q_0.p_0 - q_1.p_1 - q_2.p_2 - q_3.p_3 \\ \hline (q_0.p_1 + q_1.p_0 + q_2.p_3 - q_3.p_2).i \\ (q_0.p_2 - q_1.p_3 + q_2.p_1 + q_3.p_1).j \\ (q_0.p_3 + q_1.p_2 - q_2.p_2 + q_3.p_0).k \end{array}\right] \quad (7)$$

A rotation around the vector $\mathbf{v}$ by an angle θ on the reference frame $\langle i, j, k\rangle$ can be written q_θ [3]:

$$q_\theta = \left[\begin{array}{c} \cos\frac{\theta}{2} \\ \hline \\ \mathbf{v}.\sin\frac{\theta}{2} \\ \\ \end{array}\right] = \left[\begin{array}{c} \cos\,\theta/2 \\ \hline v_i.\sin\,\theta/2 \\ v_j.\sin\,\theta/2 \\ v_k.\sin\,\theta/2 \end{array}\right] \quad (8)$$

Which is way smaller in terms of memory usage than the equivalent 3×3 rotation matrix.

REFERENCES

[1] B. Aguilaniu, H. Roth, J. Gonzalez-Bermejo, M. Jondot, J. Maitre, F. Denis, T. Similowski. A simple semi-placed three minutes chair rise test (3CRT) for routine exercise tolerance testing in COPD. Int. Journal of COPD, 2014 (under publication)

[2] N. Noury, B. Perriot, J. Collet, E. Gre nier, M. Cerny, B. Massot, E. McAdams, ActimedARM – Design of a Wearable System to Monitor Daily Actimetry, 35th Annual International Conference of the IEEE EMBS, Osaka, 3-7 July, 2013, pp.1851-4

[3] J. Diebel, Representing Attitude: Euler Angles, Unit Quaternions, and Rotation vectors, Stanford University, Stanford (CA), 20 October, 2006

[4] L. D. Slifka, An Accelerometer based Approach to Measuring Displacement of a Vehicle Body, Master of Science in Engineering Thesis, University of Michigan, April, 2004

[5] J. Calusdian, A Personal Navigation System Based on Inertial and Magnetic Field Measurements, Naval Postgraduate School, Monterey (CA), September, 2010